Biomimetic coating of bisphosphonate incorporated CDHA on Ti6Al4V

Huan Zhou · Joseph G. Lawrence · Ahmed H. Touny · Sarit B. Bhaduri

Abstract Bi-functional coatings of carbonated calcium deficient hydroxyapatite (CDHA) on Ti alloys were developed by using a biomimetic coating process. The bi-functionality was achieved by loading alendronate sodium (AS), an approved bisphosphonate drug used for the treatment of osteoporosis, into the inner layers of CDHA coatings. Three possible methods of loading AS into CDHA coatings were systematically studied and compared. The results indicated that the co-precipitation method had greater benefits and can modify the release profile of AS by incorporating AS in the inner layers of the coatings. As a preliminary study, the influences of applied AS dosage to CDHA coatings were evaluated using XRD and SEM. In vitro tests indicated that the AS content on CDHA coatings played a significant role, and optimum AS content in local area is beneficial for osteoblast cells proliferation. It is expected that the CDHA–AS coatings via the co-precipitation approach have potential for bone tissue engineering applications.

H. Zhou (✉) · J. G. Lawrence
Department of Bioengineering, The University of Toledo,
Toledo, OH, USA
e-mail: Huan.Zhou@Rockets.utoledo.edu

A. H. Touny
Department of Chemistry, Helwan University, Ain Helwan,
Cairo, Egypt

S. B. Bhaduri
Department of Mechanical, Industrial and Manufacturing
Engineering, The University of Toledo, Toledo, OH, USA

S. B. Bhaduri
Department of Surgery (Dentistry), The University of Toledo,
Toledo, OH, USA

1 Introduction

The prime motivation behind this study is to develop bi-functional coatings of carbonated calcium deficient hydroxyapatite (CDHA) on titanium alloys. The goal is to combine the CDHA with a drug belonging to the bisphosphonate (Bp) family and achieve the bi-functionality. The most important objective of promoting osseointegration at the metal surface will be achieved by CDHA and the treatment of osteoporosis will be aided by alendronate sodium (AS) an approved drug in the Bp family. The idea is to deliver the drug locally, at an optimal level of dosage using a benign low-temperature biomimetic process.

Calcium phosphate (CaP) coatings play an important role in the success of osteointegration of metallic implants for bone tissue regeneration [1, 2]. In addition, CaP coatings can potentially work as drug-carrier system to further promote bone healing [3, 4]. However, the conventional high-temperature coating processes such as plasma spraying [1] not only lower the bioactivity of CaP materials, but also limit the possibility to incorporate bioactive agents into these coatings. Furthermore, a high temperature process removes the carbonates from the HA structure. Hence, the biomimetic coating process is a viable alternative.

Biomimetic coating technique is based on the use of simulated body fluid (SBF), with ion concentrations, temperature, and pH almost similar to physiological conditions. SBF has the ability to induce deposition of bone-like CDHA coatings on Ti and its alloys surface when suitably treated [5–7]. The chemical composition of as-deposited CDHA is relatively close to the mineral component of bone, which is poorly crystalline hydroxyapatite (HA) with small amounts of sodium (Na^+), potassium (K^+), magnesium (Mg^{2+}), chloride (Cl^-), and carbonate (CO_3^{2-}) present in the lattice structure [8–10]. It is biocompatible, bioactive, as well as

biodegradable. The extra elements in small quantities were reported to influence cell adhesion, proliferation of osteoblasts and help in bone metabolism [10].

For more than three decades, Bps have been used as primary agents for the treatment of bone related diseases such as osteoporosis [11]. All Bp drugs share the same main backbone (P–C–P) structure. This structure provides the high affinity of Bp to CaP crystals, in which the phosphoryl groups are bound simultaneously to the same calcium atom with the formation of a bidentate or possibly tridentate chelate [12]. Such high affinity, combined with its biological effects on osteoclasts and osteoblasts, makes Bp an important bioactive agent for the treatment of osteoporosis and bone regeneration. In addition, unique side chains of Bp in R1 and R2 positions determine different chemical properties: the hydroxyl group at R1 position increases the affinity of Bp to CaP crystals, while the ability to fight against osteoclast cells is related to chemical moiety in R2 position [13]. Various Bps with different side chains are available in the market including olpadronate, alendronate, zoledronate and pamidronate [11, 13].

The systemic delivery of Bps by methods such as oral administration was reported to have limitations such as low absorption in target tissue, and side effects such as gastric injury and oral ulcers [13–15]. In recent years, local delivery of Bp to the target area of bone has become popular. In the early stage of implantation during bone replacement when significant bone loss can occur, Bp can provide a stable and integrated interface between the implant and the bone [16]. For example, Tengvall et al. [17] reported a 28% increase in the pull-out force and 90% increase in pull-out energy of Bp loaded implant in rats as opposed to those without Bp. Peter et al. [18, 19] examined zoledronate loaded HA coated Ti implant, reporting excellent results in terms of bone growth around the implants, especially when the zoledronate content is optimum (between 0.2 and 2.0 μg per implant). Because of its reported effects on bone healing, it may be beneficial to incorporate Bp into CDHA coated metallic implants for bone replacement applications.

In this work, we evaluate three possible methods of loading Bp into CDHA coatings and compare them systematically. These methods include: (I) classical Bp aqueous solution contact with as-deposited CDHA coatings [18–20]; (II) co-precipitation of Bp–CDHA coatings; (III) alternative layer by layer coatings of CDHA and Bp by several cycles. The effects of coating method on the morphology of CDHA coatings were investigated and the loading and release prolife of Bp were also assessed. The best loading method was then selected and different Bp loading was used to evaluate the effects of Bp contents on CDHA coatings formation. As a preliminary study, the optimum Bp dosage to be incorporated into CDHA coatings were determined using in vitro tests on osteoblast cells.

2 Experiments

2.1 Sample pre-treatment

A Ti6Al4V plate (McMaster-Carr, CA) was cut into small strips with dimensions of $5 \times 5 \times 1$ mm, which were used as substrates for CDHA coating. The strips were polished by using #1000 silicon carbide (SiC) paper (Struers, Denmark) and cleaned using distilled water. A set of four strips were immersed in 50 ml of 5 M sodium hydroxide (NaOH) solution at 60°C for 24 h, and then re-immersed in 50 ml of distilled water for 24 h at 37°C in order to remove extra NaOH on the sample surface. NaOH was purchased from Fisher Scientific. The NaOH solution was prepared by dissolving NaOH into DI water with stirring. The purity of NaOH is listed as 99.8%. Subsequently, these strips were dried at 37°C for 24 h.

2.2 SBF preparation

The SBF used in this work was 1.5X t-SBF which is a Tris ($C_4H_{11}NO_6$) buffered SBF solution developed by our group [21, 22]. Its composition closely mimics the composition of human blood plasma. The ionic concentrations of t-SBF solution were intensified 1.5 times to accelerate CDHA coating formation. The composition is shown in Table 1. The reagents sodium bicarbonate ($NaHCO_3$) and sodium sulfate (Na_2SO_4) were purchased from Acros Organics (NJ). Sodium chloride (NaCl), potassium chloride (KCl), sodium phosphate dibasic (Na_2HPO_4), magnesium chloride ($MgCl_2 \cdot 6H_2O$), hydrochloric acid (HCl), calcium chloride ($CaCl_2 \cdot 2H_2O$), and Tris-Base buffer were purchased from Fisher Scientific (NJ). The purity of all chemicals is listed as over 99.5%. The reagents were measured with 0.002 g of error. All reagents were dissolved in 700 ml of DI water one by one in the order listed in Table 1 and extra DI water was added to make the final solution volume 1 l using a 1 l

Table 1 Compositions of 1 l 1.5X t-SBF

Order	Reagent	1.5X t-SBF (g)
1	NaCl	9.8184
2	NaHCO$_3$	3.4023
3	KCl	0.5591
4	Na$_2$HPO$_4$	0.2129
5	MgCl$_2$.6H$_2$O	0.4574
6	1 M HCL	15 ml
7	CaCl$_2$.2H$_2$O	0.5822
8	Na$_2$SO$_4$	0.1080
9	Tris-Base	9.0945
10	1 M HCl	50 ml

cylinder with 5 ml error. The solution was stored at 5°C, when not in use.

2.3 Drug loading

The FDA approved aldenaronate sodium (AS) was purchased from Fisher Scientific (NJ). Three different methods were used to load AS into CDHA coatings on Ti6Al4V via incubating strips into solution with different components (four strips in each 50 ml solution). In method I, the pre-treated Ti6Al4V substrates were soaked vertically at 37°C in 50 ml of 1.5X t-SBF solution in a tightly sealed 100 ml Pyrex glass bottles (Corning Life Sciences, MA) for 15 days to obtain the CDHA coatings. The 1.5X t-SBF solution was replenished every 48 h. The CDHA coated strips were then separated into two groups (I-1 and I-2). In group I-1, the strips were soaked in 50 ml of AS solution with a concentration of 1×10^{-4} mol/l for 6 days, with solution replenished every 48 h. In group I-2, the strips were soaked for another 5 days in 1.5X t-SBF and then immersed in AS solution with a concentration of 3×10^{-4} mol/l for 24 h. In method II, same protocol as method I was used with AS solution replaced by AS-1.5X t-SBF. Again, the coated strips were separated into two groups (II-1 and II-2). In group II-1, the strips were soaked in AS-1.5X t-SBF with 1×10^{-4} mol/l AS for 6 days. In group II-2, the strips were soaked in AS-1.5X t-SBF with 1×10^{-4} mol/l AS for 24 h. In method III, the pretreated Ti6Al4V strips were coated with 1.5X t-SBF for 24 h followed by AS solution for the next 24 h. The layer by layer coating process was continued by alternating between 1.5X t-SBF and AS solution for a total of 21 days. The total amount of AS used for each method was the same. After 21 days of CDHA coating and AS incorporation using different methods, all strips were dried in an oven at 37°C for further analysis.

2.4 Analysis

The morphology of CDHA–AS coatings formed using different methods was examined using a scanning electron microscope (SEM, S4800, Hitachi). A reverse phase high performance liquid chromatography (HPLC) protocol utilizing pre-column derivatization of the primary amine group of AS with 9-fluorenylmethyl chloroformate (FMOC, $C_{15}H_{11}ClO_2$) was used to obtain the AS release profile [23]. Chemicals for HPLC analysis: sodium citrate ($Na_3C_6H_5O_7$), sodium phosphate dibasic anhydrous (Na_2HPO_4), acetonitrile (CH_3CN), methanol (CH_3OH), dichloromethane (CH_2Cl_2), orthophosphoric acid (H_3PO_4), sodium tetraborate decahydrate ($Na_2B_4O_7·10H_2O$), and FMOC were purchased from Fisher Scientific (NJ). $Na_3C_6H_5O_7$, Na_2HPO_4, and $Na_2B_4O_7·10H_2O$ have purity above 99.0% and all liquids used are HPLC grade. 0.1 M sodium citrate solution, 0.1 M

Table 2 Compositions of 1 l PBS

Reagent	Weight (g)
NaCl	8
KCl	0.2
Na_2HPO_4	1.44
KH_2PO_4	0.24

sodium borate solution and FMOC solution (0.1%, w/v) was prepared (FMOC was dissolved in acetonitrile). Phosphate buffer solution (PBS) was prepared for AS release, the composition of PBS is outlined in Table 2. NaCl, KCl, Na_2HPO_4 and potassium phosphate monobasic (KH_2PO_4) were purchased from Fisher Scientific with purity over 99.5%. The AS-treated strips were soaked in well plates with 100 μl PBS, which was collected and replenished every 8 h. The collected solution was stored in a refrigerator at 5°C for further analysis. Some of the strips were treated with HCl in order to dissolve CDHA for further assessment of total AS loading. The chromatographic analyses were performed using the HPLC system (Agilent Technologies HPLC 1100) with a reverse phase (PRP-1) column (10 μm particle size, 250 × 4.1 mm, Hamilton, NV). The mobile phase was prepared by mixing methanol, acetonitrile and a buffer containing 0.05 M sodium citrate and 0.05 M sodium phosphate dibasic anhydrous (pH 8, adjusted using orthophosphoric acid). The volume ratio of methanol, acetonitrile, and buffer was 5:20:75. A flow rate of 0.5 ml/min was used in the HPLC at room temperature. FMOC derivative was detected using a spectrophotometric detector operated at a wavelength of 266 nm.

2.5 Preliminary evaluation of CDHA and cell proliferation

Ti6Al4V strips were coated with CDHA–AS using the optimum drug loading method based on the results obtained from prior experiments. Different AS concentrations were used to investigate the effects of resulting AS contents on CDHA coatings. AS concentrations of 0, $n \times 10^{-6}$, $n \times 10^{-5}$ and $n \times 10^{-4}$ mol/l were used, and n was 1 or 3 depending on the application procedure. The CDHA coatings on Ti6Al4V strips, formed at different AS concentrations were characterized by X-ray diffraction (XRD, Ultima III, Rigaku). For all samples, data was collected at 2θ angles ranging from 10 to 45° at a scan speed of 1° per minute. The XRD was operated at 40 kV and 44 mA with a monochromated Cu Kα radiation source. The morphology of CDHA coatings formed at different AS concentrations was examined using the SEM. The optimum AS dosage was assessed by in vitro tests using 7F2 mouse osteoblast cells (CRL-12557, American Type Culture Collection, Manassas, VA). First the cells were cultured at

37°C and 5% CO_2 in alpha minimum essential medium (α-MEM, Thermo Scientific HyClone), augmented by 10% fetal bovine serum (FBS, Thermo Scientific HyClone). The culture medium was replenished every other day until the cells reached a confluence of ~90%. A 48 well plate (Corning® cell culture plates with CellBIND® surface) was used for in vitro testing. Approximately 10,000 cells in 500 μl culture medium were seeded to each well containing the sterilized coated strip. The numbers of cells on the strips and surrounding strips in well were counted after 24 h using cytotox 96® non-radioactive cytotoxicity assay kit (Promega, WI) and after 6 days using a hemocytometer. For statistics, all cell culture experiments were performed in triplicates. The morphology of the osteoblast cells on the surface of the strips was examined using SEM after sample preparation by alcohol dehydration, critical point drying and sputter coating using gold.

3 Results

3.1 Morphology of CDHA–AS coatings using different methods

The NaOH-etched Ti6Al4V showed a porous surface morphology as seen in Fig. 1a. Both method I (Fig. 1b) and II (Fig. 1c) produced uniform CDHA–AS coatings on the surface of Ti6Al4V. These coatings were in the form of a dense layer with growth of CDHA globules on top, similar to previous work [21]. However, method III produced very thin and loose CDHA layers which were more likely the debris rather than coatings (Fig. 1d). Hence, it was evident that method III cannot produce uniform CDHA–AS coatings on Ti6Al4V.

3.2 AS release prolife

The average AS content/area of each groups are shown in Fig. 2. The AS release profiles of group I and II are shown in Fig. 3. A quick release of AS in group I-2 in PBS was observed in the first 24 h, while the release of AS in group I-1 was more stable and continuous. 80% of AS in group II-2 was released in the first 16 h as compared to a more sustained AS release prolife in group II-1. On the other hand, group II-1 also had a more stable and continuous AS release prolife as compared group I, even after 96 h.

3.3 Preliminary evaluation of CDHA and cell proliferation

Based on AS release profiles, method II-1 was selected as the preferred method and used for the preparation of CDHA–AS coatings with different AS contents. The samples prepared using method II-1 with different AS
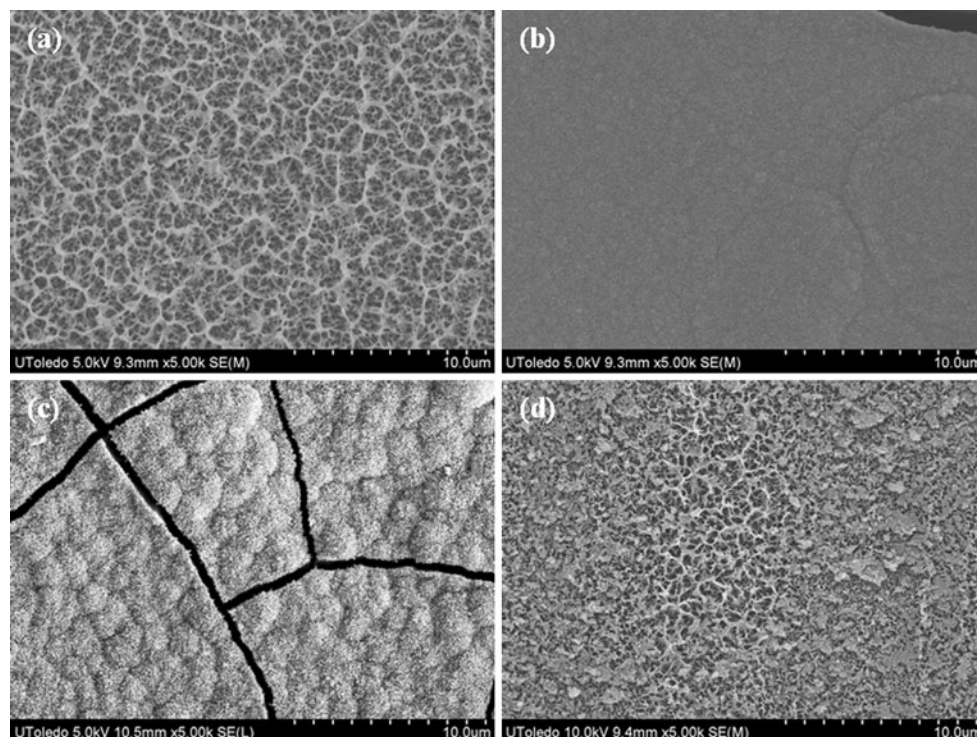

Fig. 1 SEM images of a NaOH etched Ti6Al4V surface, b AS–CDHA coatings produced using method I, c AS–CDHA coatings produced using method II, d AS–CDHA coatings produced using method III
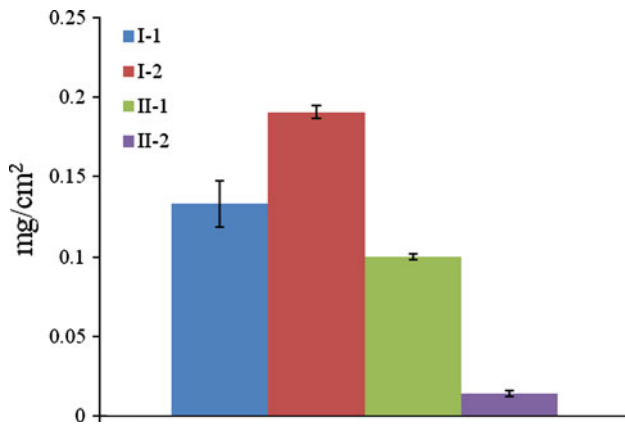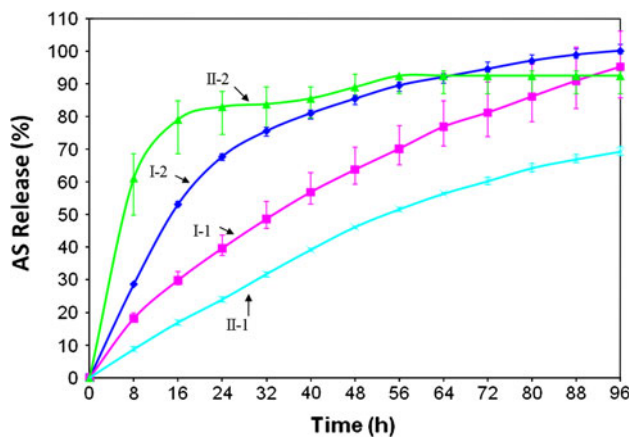
Fig. 2 The average AS content/area of each groups

Fig. 3 AS release prolife of different groups prepared using method I or II

Fig. 4 XRD patterns of samples soaked in 1.5X t-SBF solution with different concentrations of AS (0, 10^{-6}, 10^{-5} and 10^{-4} M); *A* CDHA peaks, and *squares* Ti6Al4V peaks

contents will then be used to evaluate the influence of AS content on CDHA microstructure and cell proliferation.

XRD patterns of CDHA coatings formed in 1.5X t-SBF solutions with different amounts of AS (AS concentrations of 0, 10^{-6}, 10^{-5} and 10^{-4} mol/l) are shown in Fig. 4. There are two main features observed in the XRD patterns. First, the prominent XRD peaks at 2θ angle 26 and 32° belonging to CDHA were observed on all strips (JCPDS-ICDD card no 18-03030). The deposition of CDHA on Ti6Al4V strips in presence of AS in 1.5X t-SBF is therefore confirmed. It was observed that the intensity of Ti peaks is much higher in strips formed in 1.5X t-SBF solution with 10^{-4} mol/l AS as compared to strips in conventional 1.5X t-SBF. Second, there is a broadening of CDHA peak as a function of AS content, as shown in Fig. 4.

Figure 5a through c show the SEM images from the surfaces of CDHA coatings deposited using 1.5X t-SBF solutions with different amounts of dissolved AS (AS concentrations of 0, 10^{-6}, 10^{-5} and 10^{-4} mol/l) at different magnifications. Three main features were observed in the SEM micrographs. First, in Fig. 5a all strips were found to
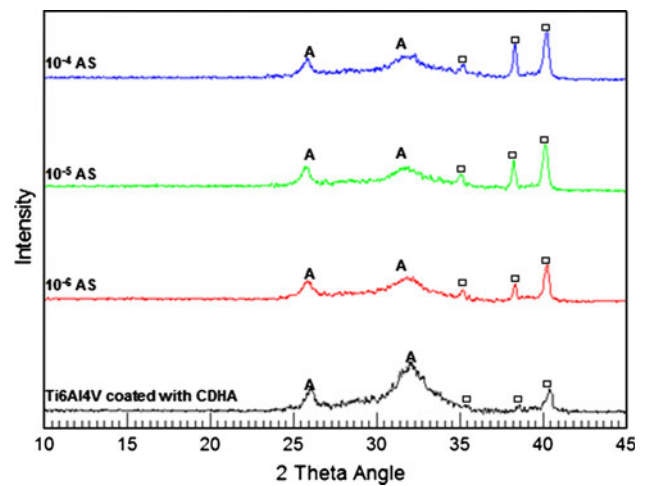
form an under-coat layer first, followed by growth of CDHA globules on it. With the decrease of AS concentrations in 1.5X t-SBF, CDHA globules number per area decreased but their size increased. Second, micro-cracks were observed on CDHA coatings precipitated from 1.5X t-SBF solutions with AS concentration of 10^{-5} and 10^{-4} mol/l. At higher magnification, the size of the micro-cracks on CDHA coatings formed in 1.5X t-SBF solution with AS concentration of 10^{-4} mol/l was observed to be much larger than ones from 1.5X t-SBF solution with AS concentration of 10^{-5} mol/l (Fig. 5b). Third, CDHA nano-crystals as shown in Fig. 5c, transformed from worm-like feature to needle-like feature as a result of increase in AS concentration.

The in vitro tests in Fig. 6a indicate that the AS content on CDHA coatings influenced osteoblast cells proliferation. After 6 days of cell culture, it was observed that the strips with coatings formed in 10^{-6} mol/l AS-1.5X t-SBF had the highest number of osteoblast cells ($P < 0.05$), and cell number decreased when AS content on CDHA coating increased. In addition, the numbers of osteoblasts surrounding strips in wells after 24 h and 6 days were shown in Fig. 6b, which also indicted the adverse effect of high content released AS to osteoblasts in the environment ($P < 0.05$). Osteoblast cell morphologies after 6 days on strips with different AS content were similar as shown in Fig. 7. The only difference is the number of filipodia (as an indicator for osteoblast cells proliferation) on coatings formed in 1.5X t-SBF with 10^{-4} mol/l AS was much lower than other strips.

4 Discussion

It is well known that a hydrated layer of sodium titanate and titanium oxide, and features of nano-scale roughness

Fig. 5 a SEM images of the surfaces of CDHA coatings deposited from 1.5X t-SBF solutions with different concentrations of AS: (*a*) 0, (*b*) 10^{-6}, (*c*) 10^{-5}, and (*d*) 10^{-4} mol/l, magnification is 1 K. **b** SEM images of the surfaces of CDHA coatings deposited from 1.5X t-SBF solutions with different concentrations of AS: (*a*) 0 (*b*) 10^{-6} (*c*) 10^{-5}, and (*d*) 10^{-4} mol/l, magnification is 5 K. **c** SEM images of the surfaces of CDHA coatings deposited from 1.5X t-SBF solutions with different concentrations of AS: (*a*) 0, (*b*) 10^{-6}, (*c*) 10^{-5}, and (*d*) 10^{-4} mol/l, magnification is 100 K
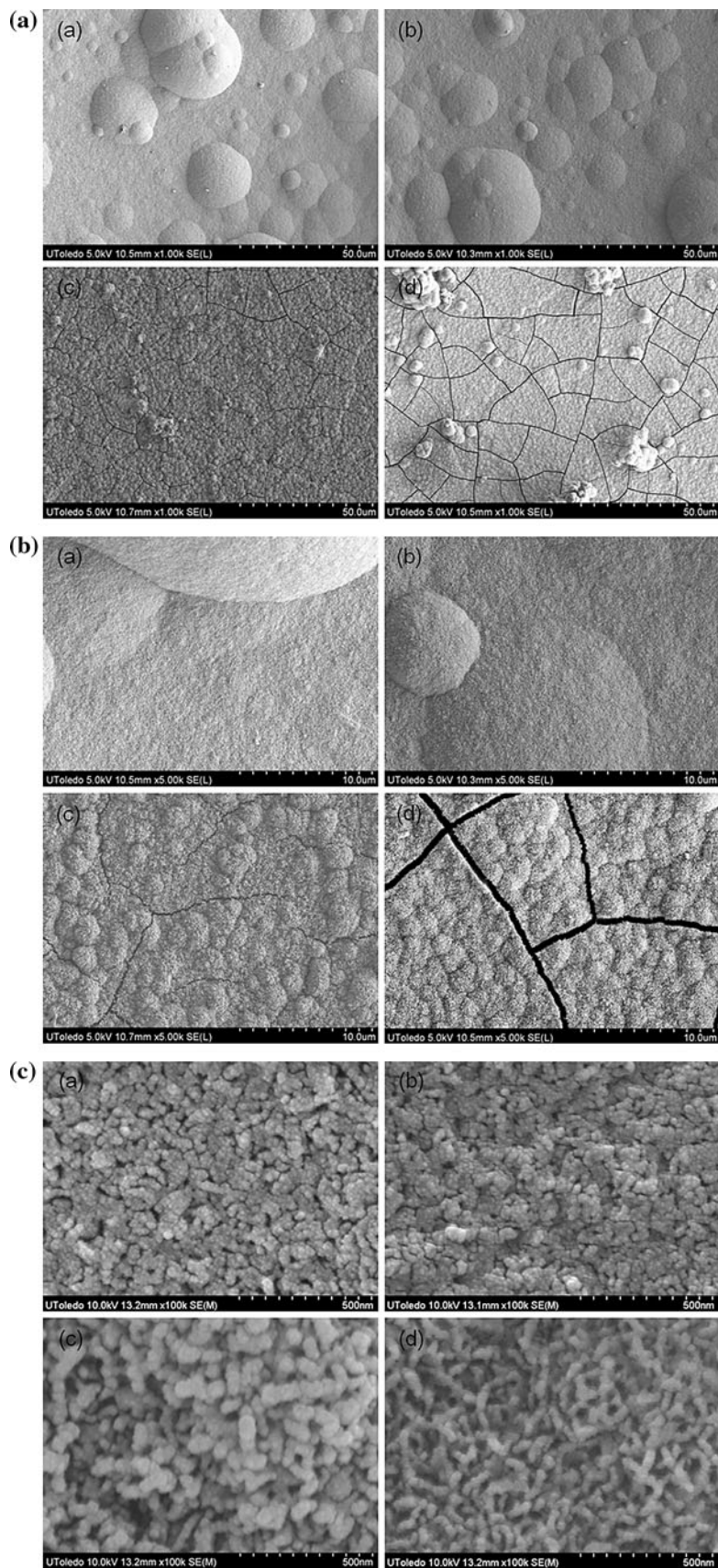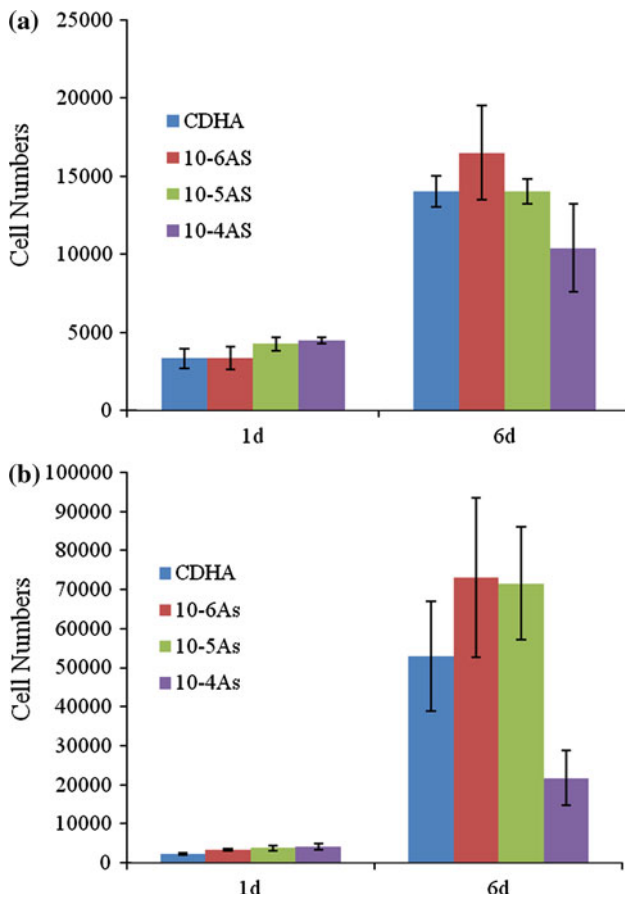
Fig. 6 **a** Osteoblast cell numbers on CDHA coatings deposited from 1.5X t-SBF solutions with different concentrations of AS: (1) 0, (2) 10^{-6}, (3) 10^{-5}, and (4) 10^{-4} mol/l after 24 h and 6 days. **b** Osteoblast cell numbers surrounding strips with CDHA coatings deposited from 1.5X t-SBF solutions with different concentrations of AS: (1) 0, (2) 10^{-6}, (3) 10^{-5}, and (4) 10^{-4} mol/l after 24 h and 6 days

can form on the exposed surfaces of Ti6Al4V substrates after 24 h of NaOH etching at 60°C [6, 24]. In this work, such phenomenon was also observed as shown in Fig. 1a. The chemically formed sodium titanate can be transformed

into Ti–OH via ion exchange of its Na^+ ions with H_3O^+ ions in the surrounding aqueous environment, and these formed Ti–OH groups can in turn react with Ca^{2+} ions present in solution to form amorphous calcium titanate, which were the sites for CDHA deposition [25]. In method I and II, a dense layer of CDHA was successfully deposited before AS incorporation. However, in method III, the situation was totally different: the CDHA deposition was obstructed when AS was incorporated in the initial step of CDHA formation. It was reported that Bp can form strong bonding to potential CaP crystal growth sites in order to block further accumulation of reactant ions from solution [26, 27]. In method III, amorphous calcium titanate was formed in the first 24 h of 1.5X t-SBF immersion. The following AS–aqueous solution treatment introduced AS to these amorphous calcium titanate as a protective layer to avoid further CDHA growth on Ti6Al4V surface. Such protective layer is not 100% inhibitory to CDHA growth because AS were randomly adsorbed on these amorphous calcium titanate sites and AS can be released back to aqueous environment. However, in method III in turns soaking Ti6Al4V in 1.5X t-SBF and AS aqueous solution intensified such inhibitory effect of AS, resulting in poor CDHA coating formation on Ti6Al4V surface. On the other hand, adsorbed AS cannot destroy formed CDHA coatings, and thus both method I and II can produce uniform CDHA–AS coatings.

CDHA is a potential carrier for AS administration. Josse et al. [28, 29] studied the delivery of zoledronate from biphasic calcium phosphate (BCP, consisting of different ratio of HA and beta-tricalcium phosphate) and calcium deficient hydroxyapatite (CDA, $Ca_{10-x}(PO_4)_{6-x}(HPO_4)_x$ $(OH)_{2-x}$). Zoledronate reportedly formed a calcium complex in the crystalline form on BCP materials while getting absorbed on CDA surface via polar covalent interactions with calcium atoms. It was indicated that CDA caused sustained release of zoledronate over a period of time as compared to fast release of zoledronate from BCP in
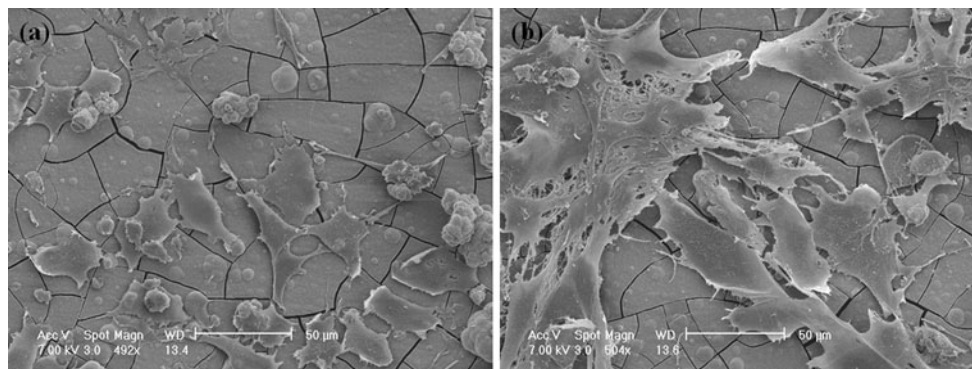

Fig. 7 SEM images of osteoblast cells on the CDHA coatings deposited from 1.5X t-SBF solutions with different concentrations of AS after 6 days: **a** 10^{-4}, and **b** 10^{-5} mol/l

biological evaluation [29]. The chemical composition of CDHA $(Ca_{10-x-y}[(HPO_4)_x(CO_3)_y(PO_4)_{6-x-y}](OH)_{2-x})$ is similar to CDA with extra carbonate elements presented in the lattice structure [21, 30], making CDHA more reactive in physiological environment. Oliveira et al. [20] produced CDHA coatings with Bp on starch-based degradable bio-materials via immersing CDHA coated material into Bp containing solution, and reported in a buffered solution with pH at 7.4 around 30% of the drug released in the first 24 h. In addition, the inhibitory effect of AS to CDHA dissolution possibly prolonged the release of AS from coatings [31, 32]. For the stabilization of the implant, it is preferred that sustained and stable release of Bp takes place from the implant. Local high Bp concentration caused by a quick release mechanism can result in cytotoxic effects to bone cells [33, 34].

In the AS release prolife study, method I and II were compared. The conceptual base of method I and II are different: method I is based on the adsorption of AS to CDHA coatings surface and method II is focusing on incorporating AS into inner layers of CDHA coatings together with CDHA precursors suspended in solution. The results demonstrated that once AS successfully incorporated into inner layers of CDHA coatings via co-precipitation (group II-1), a sustained and stable release prolife of AS can be obtained (Fig. 3). In method I, the AS release profile difference between group I-1 and group I-2 was possibly caused by the prolonged incorporation time in group I-1, enabling AS to slowly diffuse into the inner-layers of CDHA. On the other hand, the loading content difference between group I-1 and I-2 (Fig. 2) was possibly attributed to two factors: (1) higher concentration of AS intensified adsorption of AS to formed CDHA coatings, (2) bonded AS released back to aqueous environment, proportional to the time of contact with aqueous environment. In method II, AS was initially bonded to CaP precursors suspended in 1.5X t-SBF. This caused two phenomena: (1) AS inhibited the CaP precursors to bond to formed CDHA coatings, and thus decreasing loading content of AS, especially when AS concentration in the solution was high, (2) when AS inhibitory effects was lower (low AS concentration), layers of CHDA–AS can be slowly built on pre-formed CDHA coatings, which can thus produce sustained and stable release of AS. Therefore, method II-1 was considered as the best AS incorporation process among these tested methods.

The intensity of peaks of Ti6Al4V in XRD analysis was inversely proportional to the thickness of deposited CDHA coatings. The increase of Ti peaks intensity as a function of AS concentration in 1.5X t-SBF following method II-1 indicated the presence of AS in SBF delayed the growth of CDHA coatings on Ti6Al4V strips. This phenomenon matched the inhibitory effect of AS to CDHA crystals

growth. The micro-cracks formation related to AS content shown in Fig. 5a, b can also be attributed to the inhibition of CDHA bulk growth caused by AS. In CDHA deposition, CDHA precursors were deposited to random regions on the surface of formed CDHA coatings, which further worked as nucleation sites and expand CDHA coatings to overlap the gaps among different regions and finally to cover the whole surface area to form uniform coating layers. The loading of AS to these CDHA precursors or formed CDHA coatings, isolated local area into separated islands and inhibited growth of new CDHA to overlap gaps. In addition, AS suspended in aqueous solution can accumulate in the gaps to further avoid CDHA formation. The Increase in CDHA globule numbers per area and the decrease of CDHA globules size as a function of AS content indicated the fact that AS adsorption inhibited nucleation of CDHA crystals.

The phenomenon that CDHA nano-crystals transformed from worm-like feature to needle-like feature as a result of AS concentration increase shown in Fig. 5c was caused by the incorporation of AS to CaP crystal structure making rearrangements to further crystal growth. Octacalcium phosphate (OCP) is considered as an important interme-diate material in the formation of CDHA in SBF. It was argued by some groups that instead of the role of calcium titanate in CDHA nucleation, CDHA deposition can also take place via OCP and then transforms into CDHA via hydrolysis and partial dissolution of OCP [35, 36]. Once AS incorporated into the OCP structure via bonding to Ca^{2+} ions, it will interrupt the partial dissolution of OCP and the in situ reorganization of the lattice ions in the conversion of OCP to CDHA. Such interruptions were directly reflected in the particle features. In addition, the phenomenon of CDHA peak broadening as a function of AS content observed in XRD data can also be attributed to the incorporation of AS to OCP/CDHA lattice in biomi-metic coating process. The adsorption of AS modified the crystal lattice growth and resulted in the transformation of crystals from worm-like to needle-like features, making the crystal structure more amorphous. Such XRD peak broadening was reported before by Boanini et al. [37, 38] in HA synthesis together with alendronate by physical absorption. Also, based on our observations in the poor coatings formed via method III and this CDHA nano-crystals feature transformation caused by AS incorporation, it is suggested both calcium titanate and OCP play important roles in CDHA coating formation.

Kashii et al. reported the administration of alendronate to rats caused microstructure of bone matrix to become less anisotropic, leading to deterioration of bone material properties [39]. Because bone matrix anisotropy and its material property are strongly influenced by mineral ori-entation, it was supposed that alendronate obstructed the right mineral orientation formation. The AS incorporation

process via method II-1 can be considered as a in vitro model to mimic the process of bone matrix formation incorporated with AS in vivo. The results also indicated that the newly formed CDHA structure was obstructed by the adsorption of high content of AS.

The in vitro testing results (Fig. 6) indicated that low AS content in local area is beneficial to osteoblast cells proliferation, while high AS content can induce adverse effects. The SEM images (Fig. 7) also support this comment. It has been reported that micromole level concentration of AS in medium is toxic to osteoblast proliferation [31, 32]. This corroborates with the cell numbers variation related to AS concentration observed in our experiments. The round morphology of cells on strips using 10^{-4} mol/l AS indicated this incorporation concentration can trigger toxic effect to osteoblast cells.

5 Conclusion

Three possible methods of loading AS to CDHA coatings was systematically studied and compared. Co-precipitation of CDHA and AS can modify the release prolife of AS by incorporating AS in the inner layers of CDHA coatings. The effects of AS on the CDHA coatings formation were strongly influenced by the applied dosage. In vitro testing indicated low AS content in local area is beneficial to osteoblast cells proliferation. This preliminary study showed the possibility and benefits to produce CDHA–AS coatings via co-precipitation process for bone tissue engineering applications.

References

1. Narayanan R, Seshadri SK, Kwon TY, Kim KH. Calcium phosphate-based coatings on titanium and its alloys. J Biomed Mater Res B. 2008;85:279–99.
2. Le Guéhennec L, Soueidan A, Layrolle P, Amouriq Y. Surface treatments of titanium dental implants for rapid osseointegration. Dent Mater. 2007;23:844–54.
3. Liu Y, De Groot K, Hunziker EB. Osteoinductive implants: the mise-en-scene for drug-bearing biomimetic coatings. Ann Biomed Eng. 2004;32:398–406.
4. Aves EP, Estevez GF, Sader MS, Sierra JCG, Yurell JCL, Bastos I, Soares G. Hydroxyapatite coating by sol–gel on Ti6Al4V alloy as drug carrier. J Mater Sci Mater Med. 2009;20:543–7.
5. Kokubo T. Surface chemistry of bioactive glass–ceramics. J Non Cryst Solids. 1990;120:138–51.
6. Kokubo T, Miyaji F, Kim HM, Nakamura T. Spontaneous formation of bonelike apatite layer on chemically treated titanium metals. J Am Ceram Soc. 1996;79:1127–9.
7. Ma J, Wong H, Kong LB, Peng KW. Biomimetic processings of nanocrystallite bioactive apatite coating on titanium. Nanotech. 2003;14:619–23.
8. Dorozhkin SV, Epple M. Biological and medical significance of calcium phosphates. Angew Chem Int Ed Engl. 2002;41:3130–46.
9. Vallet-Regí M, González-Calbet JM. Calcium phosphates as substitution of bone tissues. Prog Solid State Chem. 2004;32:1–31.
10. Rey C. Calcium phosphate biomaterials and bone mineral. Differences in composition, structure and properties. Biomaterials. 1990;11:13–5.
11. Drake MT, Clarke BL, Khosla S. Bisphosphonates: mechanism of action and role in clinical practice. Mayo Clin Proc. 2008;83:1032–45.
12. Golomb G, Schlossman A, Saadeh H, Levi M, Van Gelder JM, Breuer E. Bisacylphosphonates inhibit hydroxyapatite formation and dissolution in vitro and dystrophic calcification in vivo. Pharm Res. 1992;9:143–8.
13. Russell RG, Rogers MJ. Bisphosphonates from the laboratory to the clinic and back again. Bone. 1999;25:97–106.
14. Elliott SN, McKnight W, Davies NM, MacNaughton WK, Wallace JL. Alendronate induces gastric injury and delays ulcer healing in rodents. Life Sci. 1998;62:77–91.
15. Gonzalez-Moles MA, Bagan-Sebastian JV. Alendronate-related oral mucosa ulcerations. J Oral Pathol Med. 2000;29:514–8.
16. Venesmaa PK, Kröger HP, Miettinen HJ, Jurvelin JS, Suomalainen OT, Alhava EM. Monitoring of periprosthetic BMD after uncemented total hip arthroplasty with dual-energy X-ray absorptiometry-a 3-year follow-up study. J Bone Miner Res. 2001;16:1056–61.
17. Tengvall P, Skoglund B, Askendal A, Aspenberg P. Surface immobilized bisphosphonate improves stainless-steel screw fixation in rats. Biomaterials. 2004;25:2133–8.
18. Peter B, Pioletti DP, Laib S, Bujoli B, Pilet P, Guicheux J, Zambelli PY, Bouler JM, Gauthier O. Calcium phosphate drug delivery system: influence of local zoledronate release on bone implant osteointegration. Bone. 2005;36:52–60.
19. Peter B, Gauthier O, Laib S, Bujoli B, Guicheux J, Janvier P, van Lenthe GH, Müller R, Zambelli PY, Bouler JM, Pioletti. Local delivery of bisphosphonate from coated orthopedic implants increases implants mechanical stability in osteoporotic rats. J Biomed Mater Res A. 2006;76:133–43.
20. Oliveira AL, Pedro AJ, Arroyo CS, Mano JF, Rodriguez G, Roman JS, Reis RL. Biomimetic Ca–P coatings incorporating bisphosphonates produced on starch-based degradable biomaterials. J Biomed Mater Res B. 2010;92:55–67.
21. Tas AC, Jalota S, Bhaduri SB. Effect of carbonate content and buffer type on calcium phosphonate formation in SBF solutions. J Mater Sci Mater Med. 2006;17:697–707.
22. Tas AC. Synthesis of biomimetic Ca–hydroxyapatite powders at 37°C in synthetic body fluids. Biomaterials. 2000;21:1429–38.
23. Şamdancıoğlu S, Çalis S, Kir S, Şumnu M. The determination of alendronate sodium in microparticular systems by high performance liquid chromatography. FABAD J Pharm Sci. 2003;28:183–92.
24. Jalota S, Bhaduri SB, Tas AC. Osteoblast proliferation on neat and apatite-like calcium phosphate-coated titanium foam scaffolds. Mater Sci Eng C. 2007;27:432–40.
25. Kokubo T, Kim HM. Bioactive metals: preparation and properties. J Mater Sci Mater Med. 2004;15:99–107.
26. Meyer JL, Nancollas GH. The influence of multidentate organic phosphonates on the crystal growth of hydroxyapatite. Calcif Tissue Res. 1973;13:295–303.
27. Åberg J, Brohede U, Mihranyan A, Strømme M, Engqvist H. Bisphosphonate incorporation in surgical implant coatings by fast loading and co-precipitation at low drug concentrations. J Mater Sci Mater Med. 2009;20:2053–61.
28. Josse S, Faucheux C, Soueidan A, Grimandi G, Massiot D, Alonso B, Janvier P, Laïb S, Gauthier O, Daculsi G, Guicheux J, Bujoli B, Bouler JM. Chemically modified calcium phosphates as

novel materials for bisphosphonate delivery. Adv Mater. 2004;16:1423–7.

29. Josse S, Faucheux C, Soueidan A, Grimandi G, Massiot D, Alonso B, Janvier P, Laïb S, Pilet P, Gauthier O, Daculsi G, Guicheux J, Bujoli B, Bouler JM. Novel biomaterials for bisphosphonate delivery. Biomaterials. 2005;26:2073–80.

30. Leventouri T, Chakoumakos BC, Papanearchou N, Perdiskatsis V. Comparison of crystal structure parameters of natural and synthetic apatites from neutron powder diffraction. J Mater Res. 2001;16:2600–6.

31. Fieisch H, Russell RGG, Francis MD. Diphosphonates inhibit hydroxyapatite dissolution in vitro and bone resorption in tissue culture in vivo. Science. 1969;165:1262–4.

32. Skrtic D, Eanes ED. Effect of 1-hydroxyethylidene-1,1-bisphosphonate on membrane-mediated calcium phosphate formation in model liposomal suspensions. Bone Miner. 1994;26: 219–29.

33. García-Moreno C, Serrano S, Nacher M, Farré M, Díez A, Mariñoso ML, Carbonell J, Mellibovsky L, Nogués X, Ballester J, Aubía J. Effect of alendronate on cultured normal human osteoblasts. Bone. 1998;22:233–9.

34. Naidu A, Dechow PC, Spears R, Wright JM, Kessler HP, Opperman LA. The effects of bisphosphonates on osteoblasts in vitro. Oral Surg Oral Med Oral Pathol Oral Radiol Endod. 2008;106:829–37.

35. Feng QL, Wang H, Cui FZ, Kim TN. Controlled crystal growth of calcium phosphate on titanium surface by NaOH-treatment. J Cryst Growth. 1999;200:550–7.

36. Lu X, Leng Y. TEM study of calcium phosphate precipitation on bioactive titanium surface. Biomaterials. 2004;25:1779–86.

37. Boanini E, Gazzano M, Rubini K, Bigi A. Composite nanocrystals provide new insight on alendronate interaction with hydroxyapatite structure. Adv Mater. 2007;19:2499–502.

38. Boanini E, Torricelli P, Gazzano M, Giardino R, Bigi A. Alendronate–hydroxyapatite nanocomposites and their interaction with osteoclasts and osteoblast-like cells. Biomaterials. 2008;29:790–6.

39. Kashii M, Hashimoto J, Nakano T, Umakoshi Y, Yoshikawa H. Alendronate treatment promotes bone formation with a less anisotropic microstructure during intramembranous ossification in rats. J Bone Mineral Meta. 2008;26:24–33.